
Gaussian Mapping for Evolving Scenes

Vladimir Yugay*

University of Amsterdam
vladimir.yugay@uva.nl

Thies Kersten*

University of Amsterdam
thies.kersten@uva.nl

Luca Carlone

Massachusetts Institute of Technology
lcarlone@mit.edu

Theo Gevers

University of Amsterdam
th.gevers@uva.nl

Martin R. Oswald

University of Amsterdam
m.r.oswald@uva.nl

Lukas Schmid

Massachusetts Institute of Technology
lschmid@mit.edu

vladimiryugay.github.io/game

Abstract

Mapping systems with novel view synthesis (NVS) capabilities are widely used in computer vision, with augmented reality, robotics, and autonomous driving applications. Most notably, 3D Gaussian Splatting-based systems show high NVS performance; however, many current approaches are limited to static scenes. While recent works have started addressing short-term dynamics (motion within the view of the camera), long-term dynamics (the scene evolving through changes out of view) remain less explored. To overcome this limitation, we introduce a dynamic scene adaptation mechanism that continuously updates the 3D representation to reflect the latest changes. In addition, since maintaining geometric and semantic consistency remains challenging due to stale observations disrupting the reconstruction process, we propose a novel keyframe management mechanism that discards outdated observations while preserving as much information as possible. We evaluate Gaussian Mapping for Evolving Scenes (GaME) on both synthetic and real-world datasets and find it to be more accurate than the state of the art.

1 Introduction

Visual mapping enables a machine to build a 3D representation of its surroundings based on its camera input. Imagine an autonomous car navigating a busy city or a robot exploring a cluttered room. For these systems to move safely and make decisions, they need a reliable understanding of their surroundings. Over the years, visual mapping systems have advanced [24, 18], learning to handle complex scenes with increasing accuracy. This capability forms the backbone for various systems from self-driving cars to virtual reality glasses, where spatial understanding is crucial for navigation, planning, and interaction.

Recent mapping systems have been enhanced with novel view synthesis (NVS) capabilities [18, 11], allowing them to generate realistic, immersive views of scenes. This allows more detailed scene exploration and supports the creation of high-quality virtual environments. These approaches typically assume that the scene is *static* such that optimization over multiple frames is well conditioned.

*Equal contribution

However, real-world environments are rarely static, but include both *short-term* dynamic effects (*i.e.* things moving *within* view of the camera) as well as *long-term* dynamics (*i.e.*, the scene evolving through changes *outside* the view of the camera). While some of the most recent NVS approaches address short-term dynamic objects [39, 33], the latter remains less explored. As a result, modern reconstruction methods with NVS capabilities struggle to capture changes as the scene evolves over time, preventing them from being deployed in long-term reconstruction pipelines.

During long-term mapping, systems must continuously update the 3D representation to capture the scene’s evolution and maintain reliable operation. This is especially challenging compared to classical *multi-session* mapping as changes can occur *at any time* during data collection. Recently, initial methods have started to address this challenge. A first approach is presented in Panoptic Multi-TSDFs [26], building semantically consistent submaps and reasoning about changes on the level of submaps. The following works [6, 21, 27] similarly focus on object-level mapping to handle evolving scenes. However, all these methods rely on map representations that cannot easily be re-rendered, preventing their use in AR/VR or digital maps where realistic rendering is essential.

This work addresses the challenge of long-term NVS mapping using 3D Gaussian Splatting (3DGS) in evolving scenes. The key insight of our approach is that environment changes are not random but typically follow semantically consistent patterns. We therefore integrate semantic consistency with the inherent properties of 3DGS to efficiently detect and adapt to environment changes in the incrementally built 3DGS model. As multi-view optimization is essential for accurate 3DGS mapping, we introduce a keyframe management method that appropriately masks stale areas in keyframes to retain useful information while accounting for changes, resulting in a well-conditioned 3DGS optimization process even in evolving scenes. We make the following contributions:

- We present GaME, the first NVS-capable mapping system for long-term evolving scenes.
- A Dynamic Scene Adaptation (DSA) mechanism to incrementally update a 3DGS model.
- An efficient keyframe management strategy for accurate 3D reconstruction through changes.
- We thoroughly evaluate GaME on synthetic and real-world data, showing a performance increase of 90+% in depth and 20+% in color rendering. We release the code open-source².

2 Related Work

3D Change Detection. The goal of change detection is to handle long-term dynamic effects, *i.e.*, changes to the scene occurring *outside* the view of the sensor. Typically, this is addressed in a *multi-session* setting. Most prominently, once a map for each session is constructed, changes can be identified through geometric *scene differencing* [1, 5, 13, 25]. To achieve an object-level change understanding, this has been extended using semantic information [14], where recent trends focus on the extraction of more specialized object features, including learned shape descriptors [29, 7, 25], neural object representations [6, 40], and language embeddings [23]. Most related to us, Lu et al. [16] recently presented a 3D Gaussian Splatting-based [12] approach by re-rendering the scene to newly collected views and using EfficientSAM [32] for 2D change detection. However, the assumption that the scene is static during each session and offline processing is highly limiting, as changes in human-centric and evolving scenes can occur *at any time* during the mapping process. Conversely, our mapping is designed to operate online and does not impose any limitations on the scene changes.

Online Long-Term Reconstruction. Recently, initial methods have started to address this more general online problem. A first approach is presented by Schmid et al. [26], which generates locally and semantically consistent submaps and incrementally reasons about changes at the submap level. Fu et al. [6] propose neural object descriptors to build an object-level pose graph and detect changes in the graph configuration. This has recently been extended with $SE(3)$ -equivariant descriptors [8]. Qian et al. [21] present a frame-to-map-tracking approach, using a probabilistic update rule to detect object-level changes, which is further extended to a variational factor-graph approach in [22]. A unified short- and long-term dynamic reconstruction formulation is presented in Khronos [27], where objects are reconstructed locally and verified for changes using a library of rays. Nonetheless, these methods rely on map representations that cannot easily be re-rendered. In contrast, GaME provides scene reconstruction capable of real-time color and depth rendering.

²Released upon acceptance.

Dynamic Gaussian Splatting. 3D Gaussian Splatting [12] has revolutionized novel view synthesis (NVS) by enabling photorealistic, real-time rendering at over 100 FPS. Compared to neural radiance fields [19], 3DGS is significantly more memory-efficient and faster to optimize. The problem of dynamic or 4D GS has attracted wide interest. A series of works [3, 17, 31, 36] optimize a canonical set of Gaussians from the initial frame and model temporal variations through a deformation field. However, these methods are limited to short video sequences, as they cannot introduce new Gaussians after the initial frame. Another class of approaches [4, 10, 35] directly models temporal Gaussians that can exist over subsets of frames. Despite their improved flexibility, these methods require offline optimization and multi-view input, making scalability a significant bottleneck for high-quality dynamic reconstruction. In contrast, our mapping operates online using only a single RGB-D camera.

Online Gaussian Mapping. Most related to us, 3D Gaussian Splatting has sparked a wave of online RGB-D mapping methods [18, 11, 34, 9, 37] that adopt 3D Gaussians as their primary scene representation. While these methods perform well in static environments, they struggle in dynamic environments. More recent approaches [33, 39] tackle *short-term* dynamics within the camera’s view by incorporating segmentation models to suppress transient objects like people or small moving elements. However, they remain limited in addressing *long-term* scene changes, as stale observations corrupt the optimization process. In contrast, GaME is designed to robustly handle evolving environments by filtering outdated information and maintaining high rendering quality throughout reconstruction.

3 Background: 3D Gaussian Splatting

3D Gaussian splatting (3DGS) [12] is an effective method for representing 3D scenes with novel-view synthesis capability. This approach is notable for its speed, without compromising the rendering quality. In Kerbl et al. [12], 3D Gaussians are initialized from sparse Structure-from-Motion points and are further optimized using differentiable rendering from multiple views. Each Gaussian is parameterized by mean $\mu \in \mathbb{R}^3$, covariance $\Sigma \in \mathbb{R}^{3 \times 3}$, opacity $o \in \mathbb{R}$, and RGB color $C \in \mathbb{R}^3$. The mean of a projected (splatted) 3D Gaussian in the 2D image plane μ^I is computed as follows:

$$\mu^I = \pi(P(T_{wc}\mu_{\text{homogeneous}})) , \quad (1)$$

where $T_{wc} \in SE(3)$ is the world-to-camera transformation, $P \in \mathbb{R}^{4 \times 4}$ is an OpenGL-style projection matrix, $\pi : \mathbb{R}^4 \rightarrow \mathbb{R}^2$ is a projection to pixel coordinates. The 2D covariance Σ^I of a splatted Gaussian is:

$$\Sigma^I = J R_{wc} \Sigma R_{wc}^T J^T , \quad (2)$$

where $J \in \mathbb{R}^{2 \times 3}$ is an affine transformation from Zwicker et al. [41], $R_{wc} \in SO(3)$ is the rotation component of world-to-camera transformation T_{wc} . We refer to Zwicker et al. [41] for further details about the projection matrices. The color C along one channel ch at a pixel i is influenced by m ordered Gaussians and rendered as:

$$C_i^{ch} = \sum_{j \leq m} C_j^{ch} \cdot \alpha_j \cdot \prod_{k < j} (1 - \alpha_k), \text{ with } \alpha_j = o_j \cdot \exp(-\sigma_j), \text{ and } \sigma_j = \frac{1}{2} \Delta_j^T \Sigma_j^{I-1} \Delta_j , \quad (3)$$

where $\Delta_j \in \mathbb{R}^2$ is the offset between the pixel coordinates and the 2D mean of a splatted Gaussian. The parameters of the 3D Gaussians are iteratively optimized by minimizing the photometric loss between rendered and training images. During optimization, C is encoded with spherical harmonics $SH \in \mathbb{R}^{15}$ to account for direction-based color variations. Covariance is decomposed as $\Sigma = R S S^T R^T$, where $R \in SE(3)$ and $S = \text{diag}(s) \in \mathbb{R}^{3 \times 3}$ are rotation and scale, respectively, to preserve the covariance positive semi-definite property during gradient-based optimization.

4 Method

GaME builds and maintains a 3D map capable of novel view synthesis of an evolving environment, *i.e.*, one where changes can occur during scanning but outside the view of the sensor at any time. An overview of our system is shown in Fig. 1. GaME processes depth and color images from an RGB-D sensor, using camera poses and panoptic segmentation from external estimators [2, 15]. For each keyframe, GaME triggers the Dynamic Scene Adaptation (DSA) module to incorporate new geometry and update stale regions. Simultaneously, the keyframe management system updates the state of the participating keyframes to ensure consistent multi-view optimization despite scene changes.

4.1 Online Mapping

We model our map as a set of 3D Gaussians $\{\mathbf{G}_i\}_{i=1}^N$. The goal is to create a map with object-level *semantic consistency* [26]. Intuitively, this reflects the prior knowledge that objects tend to move as a whole, even under partial observations of changed objects. However, directly extracting object-level submaps is challenging, as noisy observations can lead to many unnecessary object allocation and de-allocation operations [26]. This problem is exacerbated for 3DGS, where optimizing individual object clouds is difficult since the splatting mechanism (3) inherently correlates all Gaussians. Instead, we propose to build a singular 3DGS representation and extract objects on an ‘as needed’ basis during *Dynamic Scene Adaptation* (Sec. 4.2). During online mapping, we optimize the 3DGS parameters of the scene using a set of covisible keyframes for supervision, minimizing the loss:

$$L = \lambda_{\text{color}} \cdot L_{\text{color}}(\hat{I}, I) + \lambda_{\text{depth}} \cdot L_{\text{depth}}(\hat{D}, D), \quad (4)$$

where I is the original image, \hat{I} is the rendered image, D and \hat{D} are the measured and reconstructed depth maps, and $\lambda_{\text{color}}, \lambda_{\text{depth}} \in \mathbb{R}_{\geq 0}$ are loss weights. The color loss and depth losses are defined as:

$$L_{\text{color}}(\hat{I}, I) = (1 - \lambda) \cdot \frac{1}{K} \sum_p \|\hat{I}(p) - I(p)\| + \lambda(1 - \text{SSIM}(\hat{I}, I)), \quad (5)$$

$$L_{\text{depth}}(\hat{D}, D) = \frac{1}{K} \sum_p |\hat{D}(p) - D(p)|, \quad (6)$$

where K is the number of rendered pixels in the rendered image or depth map, $p \in \mathbb{Z}^2$ denotes the pixel coordinates, and SSIM is a structure similarity loss [30]. Our *Keyframe Management System* (Sec. 4.3) ensures that new keyframes are fully incorporated into the optimization process and that pixels observing inconsistent geometry are systematically excluded from the optimization process.

4.2 Dynamic Scene Adaptation

GaME addresses three potential scenarios: the addition, movement, or removal of an object. Note that movement can be decomposed into a removal, tracking, and re-addition step. While GaME can be readily combined with object re-localization techniques [29, 8, 25], tracking does not affect NVS and the problem can thus be simplified into two core operations: *Add* and *Remove*.

Add. In contrast to adding 3DGS in static scenes, in evolving scenes, it is essential to distinguish between adding new geometry for areas that were previously unseen and for objects that have newly appeared. We identify under-reconstructed regions in the image by low Gaussian opacity and high re-rendering depth loss. Formally, regions $\mathcal{R}_{\text{unobserved}}$ where new Gaussians are added are given by:

$$\mathcal{R}_{\text{unobserved}} = \{\mathbf{p} \in \mathbb{Z}^2 \mid L_{\text{depth}}(\mathbf{p}) > \theta_{\text{depth}} \wedge \alpha(\mathbf{p}) < \theta_{\text{opacity}}\}, \quad (7)$$

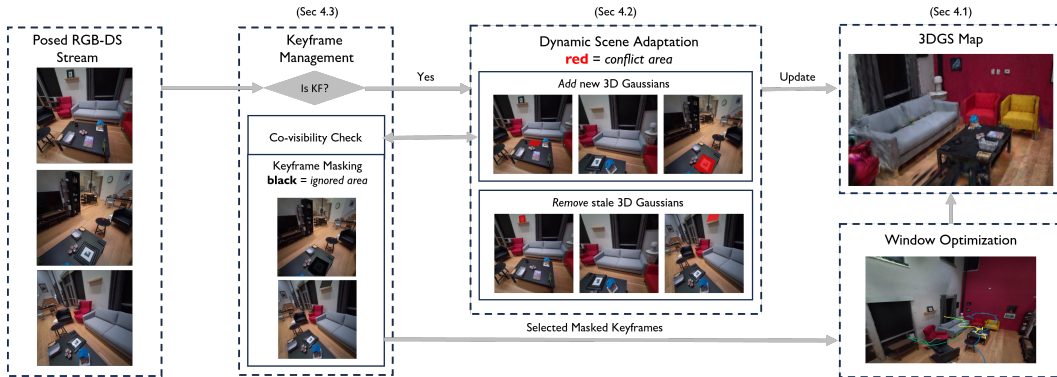


Figure 1: **GaME Architecture.** Given a segmented RGB-D input stream, the keyframe management system selects keyframes and triggers the dynamic scene adaptation (DSA) module. DSA first integrates newly observed geometry, then removes outdated geometry using covisible keyframes from the 3D Gaussian Splatting map. The keyframe manager then masks stale regions, and the mapping system uses the processed keyframes for local covisibility window optimization.



Figure 2: **Illustration of Add and Remove operations.** The input disagrees with the rendered model (red). For disappearance (top), the conflicting region is projected from previous keyframes for removal (red), where semantic consistency is enforced through the object mask (blue). This allows GaME to extract complete objects even under partial observations and occlusion. When a new object appears on the scene (bottom), new Gaussians are added (red) and the area of the new object is marked as stale in previous keyframes to prevent the contamination of the optimization process.

where $L_{\text{depth}}(\mathbf{p})$ denotes the re-rendering depth loss at pixel $p \in \mathbb{Z}^2$, $\alpha(\mathbf{p})$ represents rendered opacity, and $\theta_{\text{depth}} \in \mathbb{R}$, and $\theta_{\text{opacity}} \in \mathbb{R}$ are the respective thresholds. The method lifts the input RGB-D frame in $\mathcal{R}_{\text{unobserved}}$ to 3D and uses the resulting points to initialize the means for new Gaussians.

DSA further determines which parts of the input correspond to newly added objects, where regions of high opacity but with an input depth significantly smaller than the rendered depth indicate previously reconstructed areas occluded by newly added geometry. Formally, the set of Gaussians that might need adaptation is defined as:

$$\mathcal{G} = \{\mathbf{G}_i \mid \alpha(\mathbf{p}) \geq \theta_{\text{opacity}} \wedge \hat{D}(\mathbf{p}) > D(\mathbf{p}) + \epsilon_{\text{depth}}\}, \quad (8)$$

where $\epsilon_{\text{depth}} \in \mathbb{R}$ accounts for depth measurement noise and ensures robustness against Gaussians still converging to their final values. To enforce semantic consistency, GaME then examines each object mask of the current frame. If a sufficient portion of the mask overlaps with the rendering of \mathcal{G} , it marks the corresponding Gaussians from \mathcal{G} as needing adaptation:

$$\mathcal{G}_{\text{add}} = \left\{ \mathbf{G}_i \in \mathcal{G} \mid \frac{|\text{mask}(\mathbf{p}) \cap \text{render}(\mathcal{G})|}{|\text{mask}(\mathbf{p})|} \geq \theta_{\text{mask}} \right\}, \quad (9)$$

where $\text{mask}(\mathbf{p})$ denotes the binary mask indicating the presence of the object at pixel \mathbf{p} , and $\theta_{\text{mask}} \in \mathbb{R}$ is the overlap threshold. This further increases robustness against noisy measurements to avoid allocating spurious Gaussians or ‘floaters’.

Remove. Similarly, DSA identifies objects that have disappeared from the scene. Specifically, changed parts of the model can be identified as areas where the opacity is high (the model is well reconstructed), but the model disagrees (visually or geometrically) with the measurements:

$$\mathcal{G}_{\text{remove}} = \{\mathbf{G}_i \mid \alpha(\mathbf{p}) > \theta_{\text{opacity}} \wedge L_{\text{color}}(\hat{I}, I) > \theta_{\text{color}} \wedge \hat{D}(\mathbf{p}) < D(\mathbf{p}) - \epsilon_{\text{depth}}\}, \quad (10)$$

where $\theta_{\text{color}} \in \mathbb{R}$ is the threshold. There are two notable changes compared to the *Add* condition. First, the sign of the depth criterion is inverted, reflecting areas where the rays of the observation would penetrate into the current model, thus indicating that the model geometry can no longer be present. This also avoids spurious detections where objects are simply occluded rather than absent. Second, we leverage the high visual fidelity of 3DGS as another conflict signal by adding a color term. In contrast to most long-term mapping methods, which rely solely on 3D information [5, 25, 13, 26, 27, 22], this

allows GaME to also detect changes that are not geometrically significant, such as a sheet of paper being removed from a table. To ensure semantic consistency of removed objects, it is insufficient to rely on a single frame, as it may capture only partial views, and the object cannot be semantically detected since it is already absent. To address this, GaME renders $\mathcal{G}_{\text{remove}}$ to each covisible keyframe KF and verifies whether the color and depth are consistent with the model:

$$\mathcal{R}_{\text{remove}}^{\text{KF}} = \{\mathbf{p} \in \mathbb{Z}^2 \mid L_{\text{color}}(\mathbf{p}) > \theta_{\text{color}} \wedge L_{\text{depth}}(\mathbf{p}) > \theta_{\text{depth}} \wedge \alpha(\mathbf{p}) > \theta_{\text{opacity}}\}. \quad (11)$$

Next, each mask in the keyframe is evaluated to determine whether a significant portion intersects with the conflicting region, marking the masked Gaussians for removal:

$$\mathcal{G}_{\text{remove}}^{\text{KF}} = \left\{ \mathbf{G}_i \mid \frac{|\text{mask}(\mathbf{p}) \cap \mathcal{R}_{\text{remove}}^{\text{KF}}|}{|\text{mask}(\mathbf{p})|} \geq \theta_{\text{mask}} \right\} \quad (12)$$

Finally, the joint set, $\mathcal{G}_{\text{remove}} \cup \bigcup_{\text{KF}} \mathcal{G}_{\text{remove}}^{\text{KF}}$, is removed from the global Gaussian model. This naturally allows the extraction of individual removed objects from the global model, or deletion of the Gaussians if only an up-to-date reconstruction is desired. The DSA process is illustrated in Fig. 2.

4.3 Keyframe Management

Since jointly optimizing Gaussians using all frames from a video stream is computationally infeasible, we maintain a small window W_k of keyframes based on inter-frame covisibility. Effective keyframe management aims to select non-redundant keyframes that observe the same region while spanning a wide baseline to enforce stronger multiview constraints. In GaME, keyframes are selected every time a frame exceeds a translation $\theta_{\text{translation}} \in \mathbb{R}$ or a rotation $\theta_{\text{rotation}} \in \mathbb{R}$ threshold.

Covisibility. Upon triggering *Add* or *Remove* operations by DSA, all covisible keyframes are retrieved by reprojecting 3D points from the current frame and selecting frames where these points are not occluded. This approach differs from conventional 3DGS methods [18, 33], which determine covisibility based on the number of Gaussians used to re-render the keyframes. We found projection to be more reliable than re-rendering in multi-room environments, as Gaussians from different rooms may still appear visible due to the alpha blending, leading to erroneous covisibility estimates.

Keyframe Masking. Importantly, in evolving scenes, excluding outdated visual information is crucial, as the scene may change over time, making previous observations detrimental for the 3DGS optimization process. However, discarding entire keyframes that observe stale geometry can result in losing useful information. While some parts of the scene may change, other regions often remain stable and can provide valuable signals for 3DGS optimization. Therefore, rather than discarding entire keyframes as stale, GaME selectively ignores only the stale areas within them. To achieve this, before removing $\mathcal{G}_{\text{remove}}$ or $\mathcal{G}_{\text{remove}}^{\text{KF}}$, they are rendered onto the keyframe, and the image regions rendering them are masked out. The same procedure is applied for \mathcal{G}_{add} . Formally, the masked region \mathcal{M}^{KF} within a keyframe is defined as:

$$\mathcal{M}^{\text{KF}} = \{\mathbf{p} \in \mathbb{Z}^2 \mid \mathbf{p} \in \text{render}(\mathcal{G}_{\text{remove}}) \cup \text{render}(\mathcal{G}_{\text{remove}}^{\text{KF}}) \cup \text{render}(\mathcal{G}_{\text{add}})\} \quad (13)$$

where \mathbf{p} represents a pixel location within the keyframe, and $\text{render}(\mathcal{G}_*)$ denotes the set of pixels influenced by the Gaussian set \mathcal{G}_* when rendered. Keyframes dominated by stale regions are of little value for optimization. We exclude any keyframe in which the instance masks of objects are more than θ_{ignore} percent covered by inconsistent observations. During optimization, for all the keyframes that have ignored areas, GaME optimizes the losses:

$$L_{\text{color}}(\hat{I}, I) = \frac{1}{\sum_p \mathbb{I}[p \notin \mathcal{M}^{\text{KF}}]} \sum_p \mathbb{I}[p \notin \mathcal{M}^{\text{KF}}] \cdot \|\hat{I}(p) - I(p)\|, \quad (14)$$

$$L_{\text{depth}}(\hat{D}, D) = \frac{1}{\sum_p \mathbb{I}[p \notin \mathcal{M}^{\text{KF}}]} \sum_p \mathbb{I}[p \notin \mathcal{M}^{\text{KF}}] \cdot |\hat{D}(p) - D(p)|, \quad (15)$$

Note that compared to (5), the structure similarity term is dropped as its convolutional nature does not interact well with masking.

Refinement. An added benefit of GaME is that, optionally, the masked keyframes can be directly used for further refinement after the mapping operation, leading to consistent optimization despite changes occurring throughout the mapping stage.

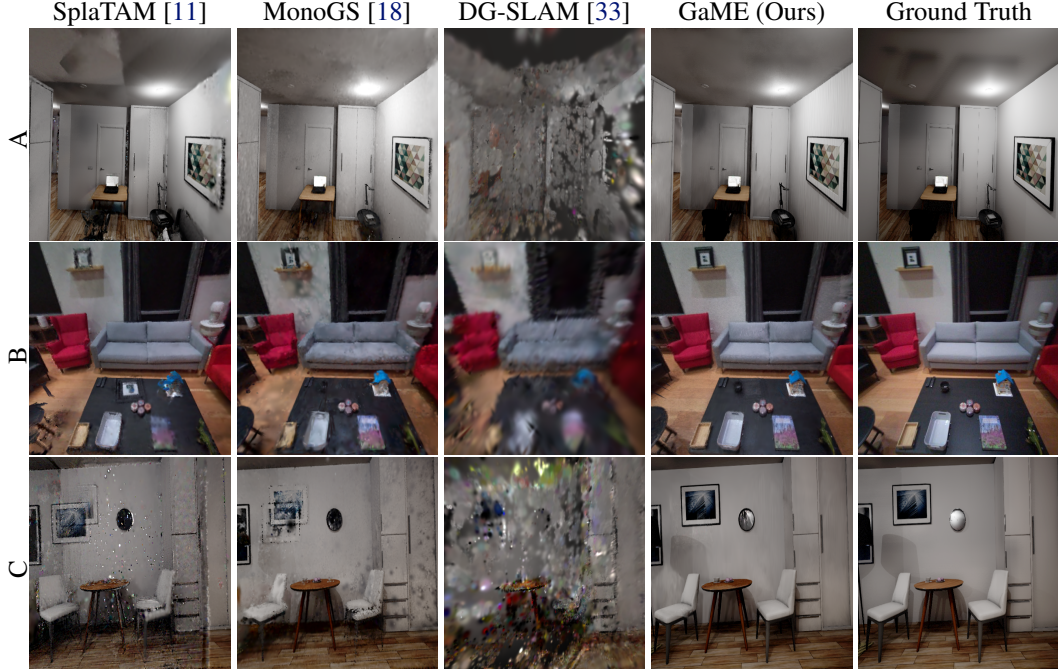


Figure 3: **Qualitative Results.** Comparison across different long-term scene changes. (A) A black office chair appears in the scene; (B) the toy house and chair are moved, the picture is moved from the table to the shelf; (C) the cutlery on the table is replaced, the painting and the right chair are moved. GaME is the only method that captures the scene evolution and preserves high rendering quality.

5 Experiments

Datasets. We test our method on the Flat [26] dataset, which consists of two RGB-D sequences captured in a synthetic environment with significant changes occurring between. We further evaluate on the Aria [20] dataset to assess performance on real-world data. We select two recordings from two rooms each that have undergone long-term changes. Finally, the TUM-RGBD [28] dataset is used to assess performance on three different static scenes following the protocol of [18].

Evaluation Metrics. To assess rendering quality, we compute PSNR, SSIM [30] and LPIPS [38]. Rendering metrics on all the datasets is evaluated by rendering full-resolution images along the ground-truth trajectory. We assess the depth error using the L1 norm in centimeters.

Baselines. We compare GaME with state-of-the-art 3DGS online reconstruction systems MonoGS [18] and SplatAM [11]. We compare to DG-SLAM [16], a recent dynamic 3DGS method, to assess the ability of dynamic 3DGS SLAM to handle evolving scenes.

Evolving Scene Evaluation Protocol. The goal of mapping evolving scenes is to render only the most up-to-date reconstruction without prior information on when the scene was changed. In addition, the system should be able to accurately render both the views it observed (input views) and unobserved frames (novel views). To achieve this, we merge RGB-D captures from every scene in the Aria and Flat datasets into a single continuous sequence to recreate this real-world behavior. For rendering evaluation, every 10th frame from each scene’s last RGB-D sequence is held out for novel view synthesis testing. The remaining 90% of frames are used to evaluate input view synthesis. To isolate the mapping performance, ground-truth poses are used for GaME and all baselines.

5.1 Evolving Scene Mapping Results

We run GaME on the Flat and Aria datasets to evaluate rendering quality in evolving scenes, shown in Tabs. 1 and 2. The Flat dataset is designed to test mapping under scene changes and includes more substantial long-term dynamics. We note that all losses are computed over complete images,

Methods	PSNR [dB] \uparrow	SSIM \uparrow	LPIPS \downarrow	Depth L1 [cm] \downarrow
SplaTAM [11]	15.88 / 12.69	0.484 / 0.299	0.548 / 0.696	21.16 / 59.91
MonoGS [18]	21.24 / 21.33	0.771 / 0.769	0.398 / 0.396	30.95 / 29.91
DG-SLAM [16]	13.72 / 13.70	0.586 / 0.603	0.737 / 0.739	73.76 / 73.90
GaME (Ours)	24.79 / 23.47	0.899 / 0.880	0.227 / 0.266	16.63 / 15.59

Table 1: **Rendering performance on the Flat dataset.** GaME shows superior performance in both color and depth rendering. Cells show metrics for input / novel views.

Methods	Scene	PSNR [dB] \uparrow	SSIM \uparrow	LPIPS \downarrow	Depth L1 [cm] \downarrow
SplaTAM [11]	room0	1.80 / 16.75	0.780 / 0.447	0.239 / 0.444	4.12 / 17.79
	room1	22.94 / 17.90	0.810 / 0.543	0.219 / 0.440	2.84 / 15.9
	Avg	22.37 / 17.33	0.795 / 0.495	0.229 / 0.442	3.48 / 16.8
MonoGS [18]	room0	25.28 / 25.19	0.781 / 0.779	0.277 / 0.273	5.15 / 5.09
	room1	23.12 / 23.02	0.844 / 0.842	0.236 / 0.241	4.99 / 5.01
	Avg	24.20 / 24.11	0.813 / 0.811	0.257 / 0.257	5.07 / 5.05
DG-SLAM [16]	room0	15.78 / 15.63	0.578 / 0.580	0.761 / 0.763	67.60 / 69.05
	room1	12.62 / 12.44	0.651 / 0.643	0.702 / 0.708	55.47 / 57.03
	Avg	14.20 / 14.04	0.615 / 0.612	0.732 / 0.736	61.54 / 63.04
GaME (Ours)	room0	28.87 / 28.94	0.934 / 0.935	0.166 / 0.166	2.3 / 2.2
	room1	30.83 / 30.54	0.961 / 0.958	0.107 / 0.114	1.8 / 1.9
	Avg.	29.85 / 29.74	0.948 / 0.947	0.137 / 0.140	2.05 / 2.05

Table 2: **Rendering performance on the Aria dataset.** GaME shows superior performance in both color and depth rendering. Cells show metrics for input / novel views.

Method	PSNR [dB] \uparrow	SSIM \uparrow	LPIPS \downarrow	Depth L1 [cm] \downarrow
No DSA	21.28 / 20.75	0.846 / 0.838	0.265 / 0.289	44.6 / 42.9
Add	24.55 / 23.37	0.900 / 0.884	0.229 / 0.268	17.9 / 17.3
Remove	24.31 / 23.14	0.896 / 0.880	0.232 / 0.267	17.6 / 16.3
Add and Remove (Ours)	24.76 / 23.47	0.898 / 0.881	0.228 / 0.267	16.9 / 15.8

Table 3: **Dynamic Scene Adaptation (DSA) ablation in the Flat dataset.** Combination of *Add* and *Remove* operations give the best performance. Cells show metrics for input / novel views.

where changed areas typically occupy a smaller part. Nonetheless, we observe notable differences in rendering performance on both datasets, where GaME is the only method that accurately adapts the reconstruction to even subtle scene changes without compromising rendering quality. This granularity is shown in qualitative results in Fig. 3. Beyond high rendering quality, GaME is able to accurately resolve changes also for challenging cases such as small cutlery on the table and flat paintings.

5.2 Ablation Studies

We conduct ablation studies to assess key design choices and analyze the reconstruction performance of both evolving and static scenes. Additional experiments on runtime and robustness to noisy input poses are provided in the Supplementary Material.

Add and Remove operations are important for Dynamic Scene Adaptation. We ablate the components of DSA in Tab. 3, showing that its presence significantly improves performance. While differences between individual DSA variants are less pronounced in final rendering quality, due to keyframe optimization correcting finer detail, combining both operations consistently yields the best performance and fastest adaptation.

Our Keyframe Management system preserves useful information. In Tab. 4, we compare keeping all keyframes against ignoring stale keyframes and ignoring only stale regions. We observe that the

Method	PSNR [dB] \uparrow	SSIM \uparrow	LPIPS \downarrow	Depth L1 [cm] \downarrow
No KF Filtering	22.29 / 21.51	0.853 / 0.853	0.254 / 0.280	30.5 / 29.5
Full KF Filtering	17.63 / 16.58	0.675 / 0.614	0.500 / 0.525	215.0 / 244.1
Partial KF Filtering (Ours)	24.76 / 23.47	0.898 / 0.881	0.229 / 0.267	16.9 / 15.8

Table 4: **Keyframe management ablation on Flat dataset.** Retaining keyframes is essential to constrain the background. However, to avoid artifacts, conflicting regions must be accurately filtered.

Method	desk	xyz	office	Average
SplaTAM [11]	20.92	21.03	21.61	21.19
MonoGS [18]	17.41	15.09	19.93	17.48
GaME (Ours)	20.94	20.54	21.96	21.15

Table 5: **Rendering performance on TUM-RGBD dataset.** GaME performs on par with state-of-the-art mapping systems for static scenes. PSNR [dB] \downarrow shown for input views.

Method	PSNR [dB] \uparrow	SSIM \uparrow	LPIPS \downarrow	Depth L1 [cm] \downarrow
No Refinement	24.48 / 23.30	0.899 / 0.883	0.231 / 0.266	17.00 / 15.90
With Refinement	24.76 / 23.47	0.898 / 0.881	0.229 / 0.267	16.90 / 15.80

Table 6: **Final refinement ablation on Flat dataset.** While refinement can potentially improve the final rendering quality, GaME already converges well during incremental processing.

naive approach to 3DGS mapping in evolving scenes by discarding conflicting keyframes can leave parts of the scene severely under-constrained, leading to the worst outcome. Ignoring changes (no filtering) achieves clear background rendering (note that the background accounts for the majority of pixels and dominates the losses), but inevitably results in artifacts and inconsistencies for changed regions, as seen in Fig. 3. Our proposed approach highlights the importance of retaining information about the background *and* resolving conflicts in keyframes for 3DGS optimization.

GaME can reconstruct static scenes. While our method is specifically designed to reconstruct evolving scenes, it should not lose the ability to reconstruct static scenes. Results on the TUM-RGBD dataset shown in Tab. 5 show that GaME performs on par with state-of-the-art systems. This suggests that the introduced DSA and keyframe management are robust to noise and false positives in model updates and masking, which could deteriorate performance.

GaME is an online mapping system. Our approach is of an incremental nature with partial optimization performed on every new keyframe. Optionally, our approach lends itself to further final refinement. Both options are shown in Tab. 6. While refinement can potentially improve the final rendering quality, we note that the model is already well converged after incremental processing.

6 Limitations

While GaME currently demonstrates robust rendering performance on evolving long-term dynamic scenes, several notable limitations exist. First, it does not yet handle short-term dynamic objects, which would result in inefficient addition and removal. Extending the dynamic scene adaptation mechanism to consider both dynamics is an exciting future direction. Second, we primarily study mapping with external pose tracking. Although sparse odometry systems can reject many changes as outliers [2], change-aware pose refinement and integration of a dedicated tracking mechanism is an exciting future direction that could improve accuracy. Third, while GaME is an online algorithm that can process sequences captured in evolving scenes, the current implementation has not been optimized for performance, which limits real-time deployment. Consistently updating the 3DGS map through incremental segmentation, rather than iterating over segmentation masks, could significantly speed up the approach. Finally, DSA is currently performed per incoming keyframe. This has the advantage of not storing semantic information in the 3DGS model and comes with some inherent robustness through the multi-view optimization process. However, individual semantic masks can be

noisy or missing, where a delayed decision or global optimization could improve performance by considering more semantic observations.

7 Conclusions

We presented GaME, the first online mapping system for evolving scenes with novel view synthesis capabilities. GaME utilizes novel dynamic scene adaptation operations to detect and correct conflicts in the incrementally built 3DGS model. Our keyframe management method furthermore appropriately ignores stale areas in keyframes, retaining useful information while correcting for changed regions, resulting in a well-conditioned 3DGS optimization process. We thoroughly evaluate our methods on synthetic and real-world datasets, demonstrating 90+% in depth and 20+% color rendering performance and artifact-free novel view synthesis in long-term dynamic evolving scenes. The code and data are released as open-source.

Acknowledgements. This work was supported by TomTom, the University of Amsterdam, Amazon, ARL DCIST program, and the allowance of Top Consortia for Knowledge and Innovation (TKIs) from the Netherlands Ministry of Economic Affairs and Climate Policy.

References

- [1] Rareş Ambruş, Nils Bore, John Folkesson, and Patric Jensfelt. Meta-rooms: Building and maintaining long term spatial models in a dynamic world. pages 1854–1861. IEEE, 2014.
- [2] Carlos Campos, Richard Elvira, Juan J Gómez Rodríguez, José MM Montiel, and Juan D Tardós. Orb-slam3: An accurate open-source library for visual, visual-inertial, and multimap slam. *IEEE transactions on robotics*, 37(6):1874–1890, 2021.
- [3] Devikalyan Das, Christopher Wewer, Raza Yunus, Eddy Ilg, and Jan Eric Lenssen. Neural parametric gaussians for monocular non-rigid object reconstruction. In *Proceedings of the IEEE/CVF Conference on Computer Vision and Pattern Recognition*, pages 10715–10725, 2024.
- [4] Yuanxing Duan, Fangyin Wei, Qiyu Dai, Yuhang He, Wenzheng Chen, and Baoquan Chen. 4d-rotor gaussian splatting: Towards efficient novel-view synthesis for dynamic scenes. In *Proc. SIGGRAPH*, 2024.
- [5] Marius Fehr, Fadri Furrer, Ivan Dryanovski, Jürgen Sturm, Igor Gilitschenski, Roland Siegwart, and Cesar Cadena. Tsdf-based change detection for consistent long-term dense reconstruction and dynamic object discovery. pages 5237–5244. IEEE, 2017.
- [6] Jiahui Fu, Yilun Du, Kurran Singh, Joshua B Tenenbaum, and John J Leonard. Robust change detection based on neural descriptor fields. In *2022 IEEE/RSJ International Conference on Intelligent Robots and Systems (IROS)*, pages 2817–2824. IEEE, 2022.
- [7] Jiahui Fu, Chengyuan Lin, Yuichi Taguchi, Andrea Cohen, Yifu Zhang, Stephen Mylabathula, and John J Leonard. Planesdf-based change detection for long-term dense mapping. *IEEE Robotics and Automation Letters*, 7(4):9667–9674, 2022.
- [8] Jiahui Fu, Yilun Du, Kurran Singh, Joshua B Tenenbaum, and John J Leonard. Neuse: Neural se (3)-equivariant embedding for consistent spatial understanding with objects. 2023.
- [9] Huajian Huang, Longwei Li, Cheng Hui, and Sai-Kit Yeung. Photo-slam: Real-time simultaneous localization and photorealistic mapping for monocular, stereo, and rgb-d cameras. In *Proceedings of the IEEE/CVF Conference on Computer Vision and Pattern Recognition*, 2024.
- [10] Kai Katsumata, Duc Minh Vo, and Hideki Nakayama. A compact dynamic 3d gaussian representation for real-time dynamic view synthesis. page 394–412, Berlin, Heidelberg, 2024. Springer-Verlag. ISBN 978-3-031-73015-3. doi: 10.1007/978-3-031-73016-0_23. URL https://doi.org/10.1007/978-3-031-73016-0_23.
- [11] Nikhil Keetha, Jay Karhade, Krishna Murthy Jatavallabhula, Gengshan Yang, Sebastian Scherer, Deva Ramanan, and Jonathon Luiten. Splatam: Splat, track & map 3d gaussians for dense rgb-d slam. In *Proceedings of the IEEE/CVF Conference on Computer Vision and Pattern Recognition*, 2024.

- [12] Bernhard Kerbl, Georgios Kopanas, Thomas Leimkühler, and George Drettakis. 3d gaussian splatting for real-time radiance field rendering. *ACM Transactions on Graphics*, 42(4), July 2023.
- [13] Giseop Kim and Ayoung Kim. Lt-mapper: A modular framework for lidar-based lifelong mapping. In *2022 International Conference on Robotics and Automation (ICRA)*, pages 7995–8002. IEEE, 2022.
- [14] Edith Langer, Timothy Patten, and Markus Vincze. Robust and efficient object change detection by combining global semantic information and local geometric verification. In *2020 IEEE/RSJ International Conference on Intelligent Robots and Systems (IROS)*, pages 8453–8460. IEEE, 2020.
- [15] Feng Li, Hao Zhang, Huaizhe xu, Shilong Liu, Lei Zhang, Lionel M. Ni, and Heung-Yeung Shum. Mask dino: Towards a unified transformer-based framework for object detection and segmentation, 2022.
- [16] Ziqi Lu, Jianbo Ye, and John Leonard. 3dgs-cd: 3d gaussian splatting-based change detection for physical object rearrangement. *IEEE Robotics and Automation Letters*, 2025.
- [17] Jonathon Luiten, Georgios Kopanas, Bastian Leibe, and Deva Ramanan. Dynamic 3d gaussians: Tracking by persistent dynamic view synthesis. In *IEEE International Conference on 3D Vision*, 2024.
- [18] Hidenobu Matsuki, Riku Murai, Paul H. J. Kelly, and Andrew J. Davison. Gaussian Splatting SLAM. In *Proceedings of the IEEE/CVF Conference on Computer Vision and Pattern Recognition*, 2024.
- [19] Ben Mildenhall, Pratul P. Srinivasan, Matthew Tancik, Jonathan T. Barron, Ravi Ramamoorthi, and Ren Ng. Nerf: representing scenes as neural radiance fields for view synthesis. *Commun. ACM*, 65(1):99–106, December 2021. ISSN 0001-0782. doi: 10.1145/3503250. URL <https://doi.org/10.1145/3503250>.
- [20] Xiaqing Pan, Nicholas Charron, Yongqian Yang, Scott Peters, Thomas Whelan, Chen Kong, Omkar Parkhi, Richard Newcombe, and Carl Yuheng Ren. Aria digital twin: A new benchmark dataset for egocentric 3d machine perception, 2023.
- [21] Jingxing Qian, Veronica Chatrath, Jun Yang, James Servos, Angela P Schoellig, and Steven L Waslander. Pocd: Probabilistic object-level change detection and volumetric mapping in semi-static scenes. 2022.
- [22] Jingxing Qian, Veronica Chatrath, James Servos, Aaron Mavrinac, Wolfram Burgard, Steven L Waslander, and Angela P Schoellig. Pov-slam: Probabilistic object-aware variational slam in semi-static environments. 2023.
- [23] Adam Rashid, Chung Min Kim, Justin Kerr, Letian Fu, Kush Hari, Ayah Ahmad, Kaiyuan Chen, Huang Huang, Marcus Gualtieri, Michael Wang, et al. Lifelong lerf: Local 3d semantic inventory monitoring using fogros2. In *2024 IEEE International Conference on Robotics and Automation (ICRA)*, pages 7740–7747. IEEE, 2024.
- [24] Antoni Rosinol, Andrew Violette, Marcus Abate, Nathan Hughes, Yun Chang, Jingnan Shi, Arjun Gupta, and Luca Carlone. Kimera: From slam to spatial perception with 3d dynamic scene graphs. *The International Journal of Robotics Research*, 40(12-14):1510–1546, 2021.
- [25] Joseph Rowell, Lintong Zhang, and Maurice Fallon. Lista: Geometric object-based change detection in cluttered environments. In *2024 IEEE International Conference on Robotics and Automation (ICRA)*, pages 3632–3638. IEEE, 2024.
- [26] Lukas Schmid, Jeffrey Delmerico, Johannes L. Schönberger, Juan Nieto, Marc Pollefeys, Roland Siegwart, and Cesar Cadena. Panoptic Multi-TSDFs: a Flexible Representation for Online Multi-resolution Volumetric Mapping and Long-term Dynamic Scene Consistency. In *2022 International Conference on Robotics and Automation (ICRA)*, pages 8018–8024, May 2022. ICRA.

- [27] Lukas Schmid, Marcus Abate, Yun Chang, and Luca Carlone. Khronos: A unified approach for spatio-temporal metric-semantic slam in dynamic environments. In *Proc. of Robotics: Science and Systems (RSS)*, 2024.
- [28] J. Sturm, N. Engelhard, F. Endres, W. Burgard, and D. Cremers. A benchmark for the evaluation of rgb-d slam systems. In *Proc. of the International Conference on Intelligent Robot Systems (IROS)*, Oct. 2012.
- [29] Johanna Wald, Armen Avetisyan, Nassir Navab, Federico Tombari, and Matthias Nießner. Rio: 3d object instance re-localization in changing indoor environments. In *Proceedings of the IEEE/CVF International Conference on Computer Vision*, pages 7658–7667, 2019.
- [30] Zhou Wang, Alan C Bovik, Hamid R Sheikh, and Eero P Simoncelli. Image quality assessment: from error visibility to structural similarity. *IEEE transactions on image processing*, 13(4): 600–612, 2004.
- [31] Guanjun Wu, Taoran Yi, Jiemin Fang, Lingxi Xie, Xiaopeng Zhang, Wei Wei, Wenyu Liu, Qi Tian, and Xinggang Wang. 4d gaussian splatting for real-time dynamic scene rendering. In *Proceedings of the IEEE/CVF Conference on Computer Vision and Pattern Recognition (CVPR)*, pages 20310–20320, June 2024.
- [32] Yunyang Xiong, Bala Varadarajan, Lemeng Wu, Xiaoyu Xiang, Fanyi Xiao, Chenchen Zhu, Xiaoliang Dai, Dilin Wang, Fei Sun, Forrest Iandola, et al. EfficientSAM: Leveraged masked image pretraining for efficient segment anything. In *Proceedings of the IEEE/CVF Conference on Computer Vision and Pattern Recognition*, pages 16111–16121, 2024.
- [33] Yueming Xu, Haochen Jiang, Zhongyang Xiao, Jianfeng Feng, and Li Zhang. DG-SLAM: Robust dynamic gaussian splatting SLAM with hybrid pose optimization. In *The Thirty-eighth Annual Conference on Neural Information Processing Systems*, 2024.
- [34] Chi Yan, Delin Qu, Dan Xu, Bin Zhao, Zhigang Wang, Dong Wang, and Xuelong Li. Gs-slam: Dense visual slam with 3d gaussian splatting. In *CVPR*, 2024.
- [35] Zeyu Yang, Hongye Yang, Zijie Pan, and Li Zhang. Real-time photorealistic dynamic scene representation and rendering with 4d gaussian splatting. In *International Conference on Learning Representations (ICLR)*, 2024.
- [36] Ziyi Yang, Xinyu Gao, Wen Zhou, Shaohui Jiao, Yuqing Zhang, and Xiaogang Jin. Deformable 3d gaussians for high-fidelity monocular dynamic scene reconstruction. In *Proceedings of the IEEE/CVF Conference on Computer Vision and Pattern Recognition*, 2024.
- [37] Vladimir Yugay, Yue Li, Theo Gevers, and Martin R. Oswald. Gaussian-slam: Photo-realistic dense slam with gaussian splatting, 2023.
- [38] Richard Zhang, Phillip Isola, Alexei A Efros, Eli Shechtman, and Oliver Wang. The unreasonable effectiveness of deep features as a perceptual metric. In *IEEE conference on computer vision and pattern recognition*, pages 586–595, 2018.
- [39] Jianhao Zheng, Zihan Zhu, Valentin Bieri, Marc Pollefeys, Songyou Peng, and Iro Armeni. Wildgs-slam: Monocular gaussian splatting slam in dynamic environments. *arXiv preprint arXiv:2504.03886*, 2025.
- [40] Liyuan Zhu, Shengyu Huang, Konrad Schindler, and Iro Armeni. Living scenes: Multi-object relocalization and reconstruction in changing 3d environments. In *Proceedings of the IEEE/CVF Conference on Computer Vision and Pattern Recognition*, pages 28014–28024, 2024.
- [41] Matthias Zwicker, Hanspeter Pfister, Jeroen Van Baar, and Markus Gross. Surface splatting. In *Proceedings of the 28th annual conference on Computer graphics and interactive techniques*, pages 371–378, 2001.

A Appendix

We provide implementation details, additional ablation studies, and qualitative results. This supplementary material includes rendered videos of reconstructed environments by GaME, compared to the baselines, on the Flat dataset, highlighting the effectiveness of our mapping approach. Additionally, we include implementation details, the ablation on sensitivity to noisy poses, and runtime analysis.

Implementation Details. In Tab. 7 we provide the hyperparameters used in our experiments.

Dataset	λ_{color}	λ_{depth}	θ_{depth}	θ_{opacity}	θ_{color}	θ_{mask}	ϵ_{depth}	θ_{rotation}	$\theta_{\text{translation}}$	θ_{ignore}
Flat [26]	1.0	1.0	4.0	0.3	0.1	0.4	2.0	50	5.0	0.9
Aria [20]	1.0	1.0	4.0	0.3	0.3	0.4	4.0	25	0.5	0.2

Table 7: Hyperparameters for Flat [26] and Aria [20] datasets.

GaME can handle noisy poses. We evaluate the camera poses on the Aria dataset with an external SLAM [18] system and use the estimated poses and keyframes instead of ground truth in Tab. 8. GaME is robust even when the pose estimation is not precise, exhibiting only a marginal performance drop under noisy pose conditions.

Camera Poses	PSNR [dB] \uparrow	SSIM \uparrow	LPIPS \downarrow	Depth L1 [cm] \downarrow
Ground-truth	26.63 / 26.71	0.920 / 0.920	0.179 / 0.180	2.4 / 2.4
Estimated	24.83 / 24.93	0.873 / 0.876	0.234 / 0.232	3.6 / 3.6

Table 8: **Usage of noisy poses on Aria room0.** GaME is robust to camera pose noise, exhibiting only a slight performance drop when using noisy poses instead of ground-truth. Camera poses and keyframes are estimated with an off-the-shelf reconstruction system [18].

Run-time Analysis. We compare the mapping runtime of our method with other state-of-the-art Gaussian-based systems in Tab. 9. Scenes with changing geometry naturally slow the mapping process, as existing methods struggle with seeding new geometry and optimizing under conflicting observations. In contrast, GaME is designed to explicitly handle such dynamic scene adaptation while being comparably efficient to the state-of-the-art mapping systems.

Metric	SplaTAM [11]	MonoGS [18]	DG-SLAM [33]	GaME (Ours)
FPS \uparrow	0.129	4.212	0.346	0.165

Table 9: **Runtime Analysis on Flat dataset.** Evolving scenes significantly slow down the mapping process. While GaME supports scene adaptation mechanisms, it performs comparably with state-of-the-art mapping systems. The frame per second is calculated by dividing the time spent on mapping by the total number of processed frames. All metrics are profiled using an NVIDIA RTX 3090 GPU.

Note on Baselines. Wild-GS [39] cannot be run with ground-truth poses, as it relies on an off-the-shelf depth estimator that may be inconsistent with them. At the same time, it fails to track the camera poses on the Aria and Flat datasets. For this reason, we were not able to compare our method with it.